

Removal of Cr (VI) from aqueous solution by activated charcoal derived from *Sapindus trifoliata* L fruit biomass using continuous fixed bed column studies

Samir Mohanta^a, Manoj Kumar Sahu^a, Prakash Chandra Mishra^b and Anil Kumar Giri^{b,*}

^a School of Engineering & Technology (BSH), GIET University, Gunupur, Odisha, India

^b Department of Environmental Science, Fakir Mohan University, Balasore, Odisha 756020, India

*Corresponding author. E-mail: anilchemnit@gmail.com

ABSTRACT

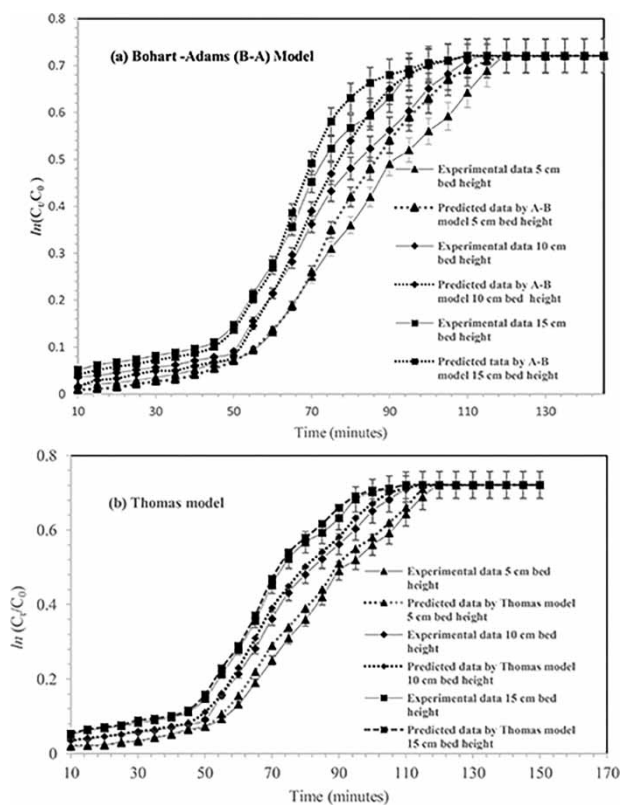
In this study, the removal of hexavalent chromium from aqueous solution were examined using activated charcoal derived from *Sapindus trifoliata* L fruit biomass in continuous fixed-bed column studies. The activated *S. trifoliata* L fruit charcoal was prepared by treating the fruit powder using concentrated nitric acid solution. Experiments were performed to investigate the effect of bed height and initial concentration on the breakthrough and saturation times. The breakthrough and saturation time increases with increase in bed height and initial concentration of chromium solutions. The maximum adsorption capacity of *S. trifoliata* L charcoal for hexavalent chromium was found to be 1.719 mg/g in the bed height 15 cm and initial concentration 10 mg/L, respectively. Column data required at various conditions were explained using Bohart-Adams and Thomas model. Two models were found to be suitable to describe the definite part of the dynamic behaviour of the column with regard to bed-height and initial concentration of hexavalent chromium. On comparison of Adjusted R^2 and estimated standard error, the Thomas model was found to best-fitted model and can be used to predict the adsorption of the hexavalent chromium in fixed-bed column studies. Activated *S. trifoliata* L fruit charcoal was characterised by SEM-EDX and FTIR analysis.

Key words: bed height, Bohart-Adams model, fixed bed column, hexavalent chromium, Thomas model

HIGHLIGHTS

- Fixed bed column adsorption is a potential technology for removal of toxicants from water.
- The maximum adsorption capacity of charcoal was found to be 1.719 mg/g.
- Activated *S. trifoliata* L fruit charcoal was characterised by SEM and FTIR analysis.
- *S. trifoliata* L fruit charcoal is low-cost with considerable high adsorption capacity.
- Thomas model was found to be the best-fitted model to predict the fixed bed adsorption.

GRAPHICAL ABSTRACT



INTRODUCTION

The rapidly progress in urbanization and industrialization is the major factors for pollution load in the natural environment. Pollutants may consist of heavy metal ions or toxic chemicals in soluble form and greenhouse gases, acid precursors, ozone depletions substances, etc. In order to maintain the ecological balance, scientists are making all out efforts to either decrease the emission of pollutants at the source or undertake measures for removal of pollutants after discharge (Nguyen *et al.* 2013; Saravanan *et al.* 2017). Among several toxic heavy metals discharged into the environment and several water bodies thus causing pollution, chromium and fluoride has become a serious health concern. Chromium ions present in both Cr^{3+} and Cr^{6+} forms in aqueous medium. The two-oxidation states of chromium have different chemical, biological and environmental characteristics (Tu *et al.* 2020). Chromium trivalent is generally insoluble in aqueous condition and necessary for microbes in few amounts as a trace metal nutrient. Hexavalent chromium usually soluble in water is a great concern due to its toxicity. Chromium is used in a variety of industrial applications and large quantities of chromium are discharged into the environment (Gupta & Babu 2009; Escudero *et al.* 2017). Present researcher study reports reveal hexavalent chromium is one of the important toxic pollutants generated by pigment production, leather industry, electroplating industry, equipment manufacturing and mining effluent activities discharged into the environment. Chromium is also found in mine water of chromite mines (Sharaf EI-Deen & Sharaf EI Deen 2015). The tolerance limit for Cr(VI) for in potable water is 0.05 mg/L (EPA 1990; Kotas & Stasicka 2000). The chromium ions presenting wastewater can be examined by various researchers using different techniques such as solvent extraction, ion exchange resin, electrochemical precipitation, biosorption, emulsion per traction technology etc (Ortiz *et al.* 2003; Singha & Das 2011; Giri *et al.* 2012; Gorzin *et al.* 2018). Some of these techniques suffer from different disadvantages such as high energy requirements, incomplete metal removal, high capital and operation cost, high cost of reagent use and tolerance to pH change. The main advantages of this technique are generally reusability of material, simple process, easy operation, eco-friendly, improved selectivity for specific metals of interest, removal of heavy metals from effluent irrespective of toxicity, and naturally aesthetic control steps for our countries. Activated carbon prepared from *Sapindus trifoliata* L fruit biomass, and its use for the removal of Cr(VI) ions from water has not been reported. In view

of the above facts it is worth to prepare the activated carbon from the fruit biomass and subsequently use the material to remove the Cr (VI) from water. Various non-conventional adsorbents removal efficiencies towards adsorbate depending upon the particle size of the adsorbent, characteristics of the adsorbent and concentration of the adsorbate. In this research, the efficiency of activated *S. trifoliata* L fruit charcoal in the removal of Cr (VI) from aqueous solution is investigated. A comparative column study has been done on the adsorption capacity of activated *S. trifoliata* L charcoal at different bed height and initial concentrations. The activated *S. trifoliata* L fruit charcoal with and without treatment of chromium ions characterized by SEM-EDX and FTIR to know the adsorption of chromium ions.

MATERIALS AND METHODS

Adsorbent preparation

Adsorbent was prepared by chemical carbonization of the *S. trifoliata* L fruit which was collected from a local market, Remuna, Balasore, Odisha. 10 g of *S. trifoliata* L fruit powder was added to 11 mL (98% m/m) of sulphuric acid and after 10 min 6.6 mL of concentrated nitric acid (65% m/m) was added to the mixture. Black slurry was transferred to the muffle furnace at 500 °C. After 1 h the activated fruit biomass converted in to activate *S. trifoliata* L fruit charcoal. The activated fruit biomass charcoal was then washed by distilled water and neutralized by 0.1N HCl and 0.1N NaOH by using pH meter. Then the activated *S. trifoliata* L fruit charcoal was dried at 110 °C in an oven after that it was crushed by motor pestle to powder. The powder was sieved and collected with desired particle size. Figure 1 shows the details preparation procedure of activated *S. trifoliata* L fruit charcoal. The physic-chemical parameters of the activated fruit charcoal results are presented in Table 1.

Preparation of standards and hexavalent chromium analysis

A stock solution of 1,000 ppm chromium (VI) was prepared by dissolving 2.83 g of potassium dichromate $K_2Cr_2O_7$ in 1 L of distilled water. By diluting this solution, standard solution of 2, 4, 6, 8 and 10 ppm was prepared for calibration purposes. It was prepared by pipetting 0.2, 0.4, 0.6, 0.8, and 1.0 mL of standard solution into five different 100 mL volumetric flasks and diluting it to 100 mL with distilled water. The details of preparation and procedure of chromium standard solution was made using manuals of standard methods for water and wastewater (Greenberg *et al.* 2005). After preparation of standard solution

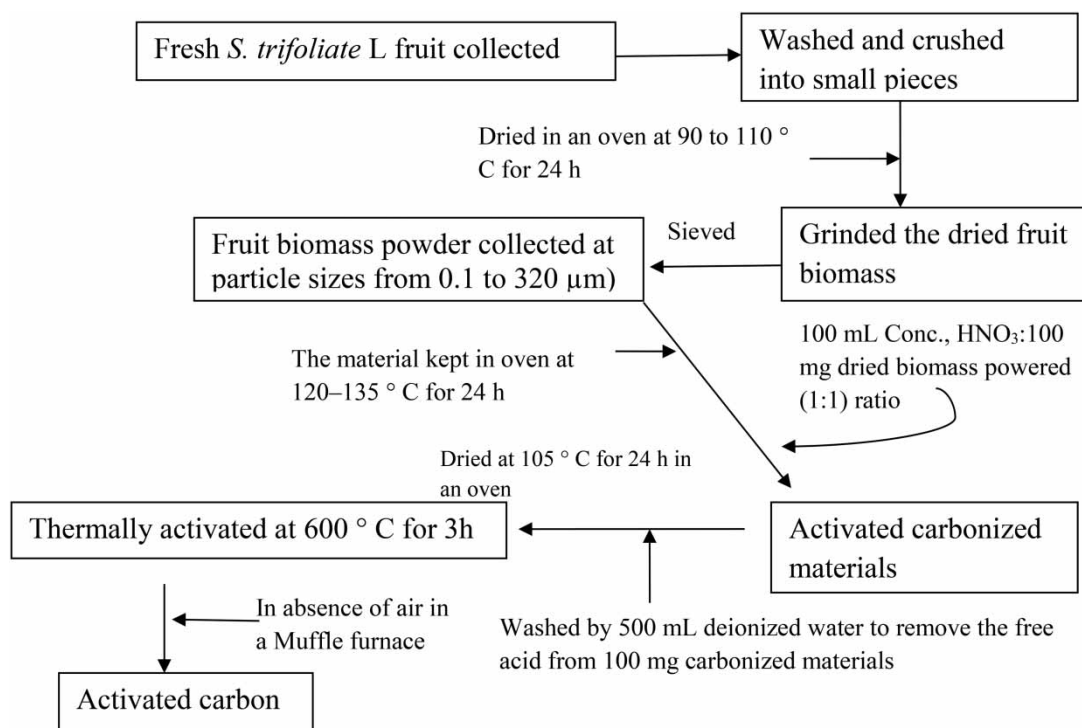


Figure 1 | Preparation procedure flow chart of activated charcoal derived from *S. trifoliata* L fruit biomass.

Table 1 | Physico-chemical parameters of the activated charcoal derived from *S. trifoliata* L fruit biomass

Parameter	Value
Carbon particle size (μm)	100–250
pH	7.2
Moisture contained (%)	10.21
Conductivity ($\mu\text{S cm}^{-1}$)	25.13
Specific gravity	0.61
Porosity (%)	75
Bulk density (g/mL^{-1})	0.65
Ash contained (%)	1.32
Ion exchange capacity (meq./g)	0.81
Water soluble matter (%)	1.76
Acid soluble matter (%)	6.11
Volatile matter (%)	45
Surface area (m^2/g)	201.11
Fixed carbon (%)	70.38

and hexavalent chromium adsorption by *S. trifoliata* L fruit charcoal, work was carried out. After stirring, the treated solutions were allowed to settle for 10 min and the samples were centrifuged at 3,000 rpm for 20 min and filtered through Whatman 42 filter paper. The filtrate was used for the analysis of residual Cr(VI) concentration in the solution. For each experiment, the concentrations of the metals before and after adsorption were determined by flame atomic absorption spectrophotometer (Perkin-Elmer P 200, USA). Same procedure was adopted in different concentration of each sample. Characterization of adsorbents before and after adsorption of chromium ions was investigated using a scanning electron microscope–energy dispersive X-ray (SEM-EDX) (JOEL model JSM-6480 LV, Japan). Fourier transform infrared (FTIR) spectra of the samples with different concentration of chromium ions were obtained by using PerkinElmer Spectrometer Spectrum RX-I. The specific surface area of activated fruit charcoal was found to be $201.11 \text{ m}^2/\text{g}$, (Brunauer-Emmett-Teller surface area analyzer, Quantachrome AUTOSORB-1, USA). This indicates that at higher temperature the volatile matter escapes from the biomass making the material porous in nature.

Adsorption modelling for fixed-bed column studies

Dynamic column studies were carried out in a glass column of 2.54 cm internal diameter and 20 cm height. A burette was used to maintain the desired flow rate. In the bottom, side of the glass a filter paper was placed to prevent any loss of adsorbent. The whole experiment was carried out at room temperature, i.e. at $30 \pm 2^\circ\text{C}$. Effect of process parameters like bed height was varied as 5, 10, and 15 cm, and initial hexavalent chromium concentration was 10 ppm with constant flow rate of 0.5 mL/min were investigated. Samples were collected every half an hour from the bottom of the column and were tested to know the hexavalent chromium concentration. The column performance was investigated by calculating the breakthrough time and adsorption capacity (Chen *et al.* 2012).

$$q_B = \left(\frac{x}{m}\right)_B = \frac{x_B}{m_{\text{adsorbent}}} = Q_v \left(C_0 - \frac{C_B}{2}\right) \frac{t_B}{m_{\text{adsorbent}}} \quad (1)$$

where C_0 is influent concentration (mg/L), x_B is the mass of chromium ions adsorbed in the column at breakthrough (mg), $m_{\text{adsorbent}}$ is the mass of the adsorbent in the column (g), Q_v is the flow rate (mL/min), C_B is the breakthrough chromium ion concentration (mg/g) and t_B is the time to breakthrough (min). A continuous adsorption separation technique needs to design data, which may be purpose of determining the conditions for an optimum performance. The optimum adsorption capacity of an adsorbent is also necessary in designing the column. The fundamental equations for a fixed-bed column are dependent on the mechanisms responsible for the process such as mass transfer from the liquid to the solid surface and diffusion and/or

reaction on the solid surface. Different simple mathematical models were developed to predict the dynamic behaviour of the column at different bed height and initial chromium concentrations in constant flow rate.

Bohart-Adams model

Bohart and Adams first proposed this model because of surface reaction theory and equivalent to the logistic curve. The rate of the adsorption was proportional to the fraction of adsorption capacity remained on the adsorbent. Bohart and Adams proposed the fundamental equation the relationship between C_t/C_0 and t in a continuous system for the adsorption of metal ions on charcoal. The equation of Bohart-Adams model (Calero *et al.* 2009; Debnath *et al.* 2010) can be expressed as:

$$\ln\left(\frac{C_t}{C_0}\right) = K_{AB} C_0 t - K_{AB} N_0 \left(\frac{Z}{U}\right) \quad (2)$$

Influent and effluent concentrations (mg/L) are denoted as C_0 and C_t . K_{AB} represent the kinetic constant (mg/L), N_0 is the saturation concentration (mg/L), t is the flow time (min), Z stands for bed depth of fixed-bed column (cm), and U is the linear flow rate (mL/min). A plot of $\ln(C_t/C_0)$ versus t gives the value of correlation coefficients (R^2), K_{AB} and N_0 by fitting the Equation (2) to the experimental breakthrough curve by applying the non-linear regression method. The value of maximum adsorption capacity can be calculated from the model using equation as follows:

$$q_0 = \frac{NoZS}{X} \quad (3)$$

where S stands for bed cross section area (cm^2) and X stands for unit mass of adsorbent packed in the column (g).

Thomas model

The Thomas model is most important and widely used theoretical methods to describe column performance. This model was assumes Langmuir kinetics of adsorption-desorption and no axial dispersion. It was assumption the rate driving force obeys second order reversible reaction kinetics (Suksabye *et al.* 2008). This model can be described by the following expression:

$$\frac{C_t}{C_0} = \frac{1}{1 + \exp\left(\left(\frac{K_{th}}{F}\right)(q_0 X - C_0 V_{ef})\right)} \quad (4)$$

where C_0 and C_t are the influent and effluent concentration (mg/L), K_{th} is the Thomas rate constant (mL/mg/min), q_0 is the maximum capacity of adsorption (mg/g), X quantity of adsorbent in the column (g). V_{ef} is volume of solution (mL) and F is the flow rate (mL/min). The values of K_{th} and q_0 can be evaluated from a plot of C_t/C_0 against t by fitting Equation (4) using non-linear regression analysis as the values of C_t/C_0 are within 0.05–0.95.

Error analysis

The model performance was evaluated through Goodness of Fit measure values adjusted R-square (R^2) and root-mean square error. The adjusted co-efficient of determination which generally takes into account the number of variables and sample size in the model. The predictive indices were calculated by using the following equation.

$$\text{Adj. } R^2 = 1 - \frac{\sum_{i=1}^n (q_{e \text{ model}} - q_{e \text{ experimental}})^2 / n - p}{\sum_{i=1}^n (q_{e \text{ model}} - q_{e \text{ experimental}})^2 / n - 1} \quad (5)$$

$$\text{RMSE} = \sqrt{\frac{1}{n - p} \sum_{i=1}^n (q_{e \text{ model}} - q_{e \text{ experimental}})^2} \quad (6)$$

RESULTS AND DISCUSSION

Characterization of treated activated charcoal

The surface morphology of activated charcoal derived from fruit biomass without and with removal of chromium ions during sorption process was observed with the help of SEM-EDX analysis. Figure 2(a) reveals different voids on the surface of charcoal without removal of chromium ions. Figure 2(b) shows the morphological changes with respect to shape and size of the materials after adsorption of chromium ions. It can be clearly observed that the surface of materials shape has been changed into new bulky particles and blackish patch structure. The EDX spectra of the chromium ions without and with adhere are shown in Figure 2(a) and 2(b). So, it was concluded that, chromium ions were adsorbed on the surface of the materials. These results are further confirmed with the FTIR spectra analysis.

FTIR spectra of the activated charcoal after experiments of 5 cm, 10 cm and 15 cm bed height a constant initial concentration of chromium solutions displays same number of absorption peaks indicates the complex nature and represented in Figure 3. The broad absorption spectra at $3,244.77\text{ cm}^{-1}$ due to bonded $-\text{OH}$ stretching vibration may be possibly complexation of $-\text{OH}$ groups with chromium ions (Owalude & Tella 2016). The absorption peak appear at $1,637.95\text{ cm}^{-1}$ may be due to $\text{C}=\text{O}$ stretching vibration of carboxylic with chromium ions (Dong *et al.* 2011). The absorbance peaks at $1,473.30\text{ cm}^{-1}$ attributed due to $\text{N}-\text{H}$ stretching vibration, $-\text{CH}_2$ scissoring or $-\text{CH}_3$ anti symmetrical bending vibration and $\text{O}-\text{H}$ deformation is shifted to lower frequency may be due to the complexation of chromium ions (Sawalha *et al.* 2007). Other peaks at $1,231.24\text{ cm}^{-1}$ and $1,069.70\text{ cm}^{-1}$ may be due the interaction of nitrogen from amino group with chromium ions (Norouzi *et al.* 2018). Another weak absorption peak at 809.43 cm^{-1} corresponds to the thiol groups with chromium ions (Yang *et al.* 2015). This clearly informed the binding of chromium ions to the treated activated charcoal.

Effect of bed height and initial concentration of a continuous fixed column studies

The bed height is one of the most important factors affect the adsorption of chromium ions in the continuous fixed bed column system. The breakthrough curve was expressed the ratio of inlet initial concentration of chromium solutions (C_t/C_0) against the flow time (t). The continuous fixed bed column adsorption studied of $\text{Cr}(\text{VI})$ ions at different bed heights (5 cm, 10 cm, and 15 cm) a constant initial concentration 10 mg/L and flow rate 0.5 mL/min, neutral pH, temperature $30\text{ }^\circ\text{C}$ and results are presented in Figure 4. Table 2 shows mathematical results of breakthrough curve and saturation time increases with increase in bed height and contact time of chromium solutions. The contact time up to 60 min with the reduction in bed height resulted in lower removal of chromium ions. The length of the bed height strongly influenced the column breakthrough time and adsorbent performance. The increase in chromium ions removal capacities with the increase in the bed height in the continuous fixed bed column because the number of binding sites increases with respect to the increase of adsorbent dose and the improved surface area of the adsorbent which delivered more binding sites for the adsorption (Baral *et al.* 2008; Chen *et al.* 2012; Yan *et al.* 2017).

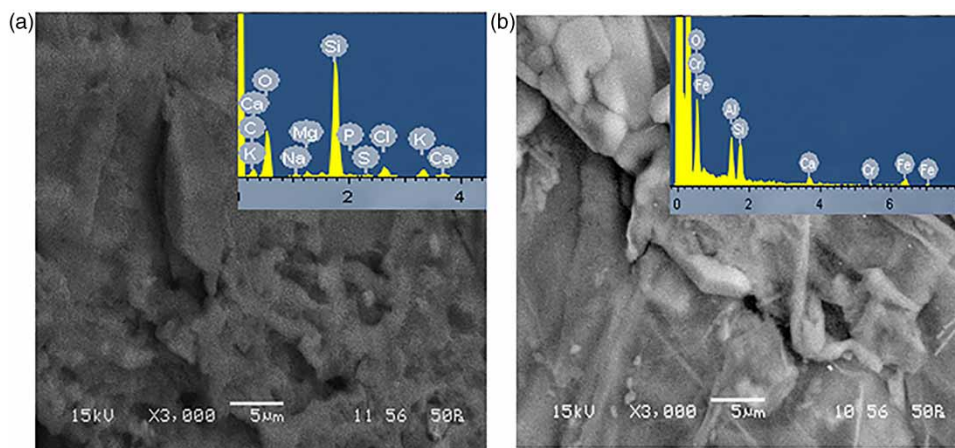


Figure 2 | SEM-EDX images of the activated charcoal (a) without (control) and (b) with (10 mg/L) chromium ions after treated 15 cm of bed height.

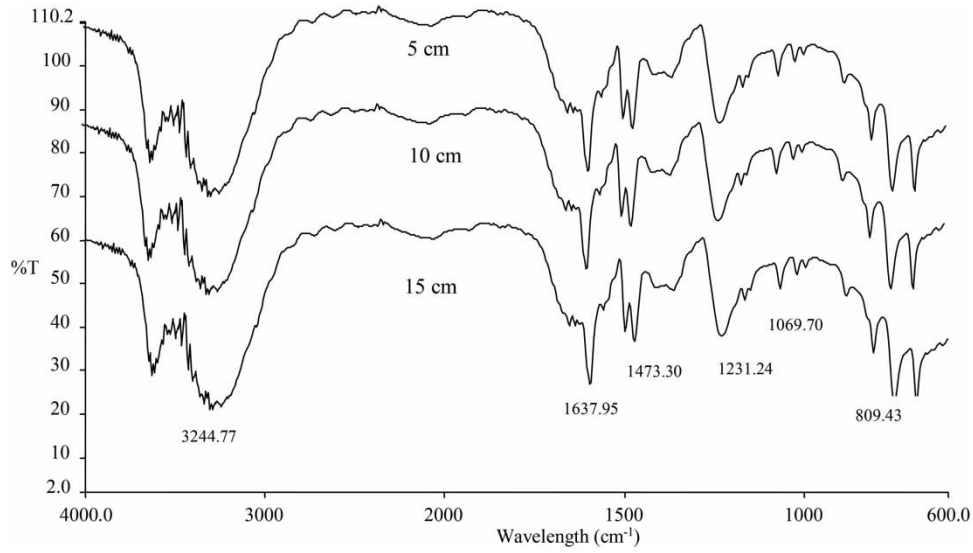


Figure 3 | FTIR spectra of the activated charcoal with different bed height a constant initial concentration 10 mg/L of chromium solutions at pH 7.

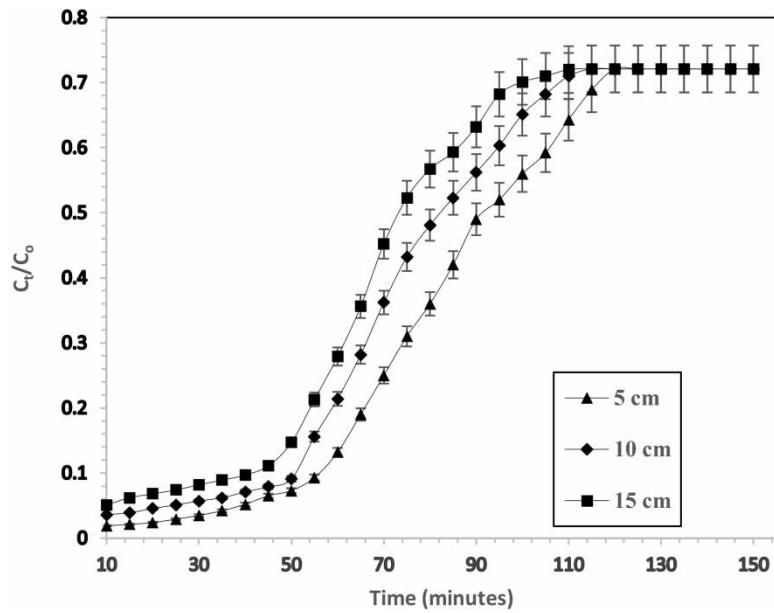


Figure 4 | Effect of bed height on the removal of Cr(VI) in the fixed bed column (Initial concentration: 10 mg/L; flow rate: 0.5 mL/min; pH: 7 and temperature: 30 °C).

Table 2 | Mathematical results of fixed bed column parameters

C_0 (Initial concentration mg/L)	Bed height (cm), Z	Qv (Flow rate mL/min)	pH	$m_{adsorbent}(g)$	$V_B(mL)$	$t_B(min)$	$C_B(mg/L)$	$q_B(mg/g)$
10	5	0.5	7	1.209	207	30	0.6	1.204
10	10	0.5	7	1.812	210	60	0.9	1.581
10	15	0.5	7	2.989	205	120	2.9	1.719

Adsorption modelling for breakthrough curve

Bohart-Adams model

Bohart-Adams model was implemented to the experimental data for describing the initial part of the breakthrough curve. This model predicted the fixed bed column performance parameters maximum saturation concentration of the chromium ions (N_0) and Bohart-Adams rate constant (K_{AB}) along with bed height, flow rate and initial chromium ions concentration of the fixed bed column system and results are presented in Table 3. The results were shows that not suitable fits with correlation coefficient ranging (0.915–0.961), Adjusted R square ranges from (0.902 to 0.953) and root mean square error ranging from (0.121 to 0.231). The effect of breakthrough curves predicted from Bohart-Adams model were compared with the experimental data with different bed height and constant initial concentration 10 mg/L and results are presented in Figure 5(a). It was very clear from Figure 5(a) and Table 3 shows a poor agreement between the experimental points and predicted values. It signified that Bohart-Adams model was unable to predict the initial process of the fixed bed column system at all working conditions (Calero *et al.* 2009). In the present study, the saturation concentration (N_0) values decreased with the increase in the bed height due to more sites are vacant for adsorption of chromium ions. These findings revealed that the adsorption process was contributed by the physical mass transfer of the column system. The Bohart-Adams rate constant K_{AB} increased (Table 3) with the increase in bed height revealed that the overall system kinetics was dominated by external mass transfer in the initial part of the column system (Chen *et al.* 2012). Therefore under these conditions, initial chromium ion concentration need to the lower kinetic constant. Finally, Bohart-Adams model operated a simple and comprehensive approach for estimating the adsorption of chromium ions.

Thomas model

Thomas model was used to predict the fixed bed column performance parameters. Thomas rate constant (k_{TH}), maximum solid-phase concentration (q_0), bed height, flow rate and initial chromium concentration of the column system and the results are presented in Table 3. The results this model shows that a suitable fits with correlation coefficient ranges (0.971–0.997), Adjusted R square ranges from (0.966 to 0.992) and root mean square error ranging from (0.213 to 0.359). The breakthrough curves predicted from Thomas model were compared with the experimental points and results are presented in Figure 5(b) and Table 3. The graphical and tabulated results show that a suitable agreement between experimental results and predicted values proposes the Thomas model. The results reveals increase of bed height with increasing the Thomas rate constant (K_{th} mL/mg/min) because of the increase in mass transport resistant with increase in the bed height. The mass transport resistance was proportional to the axial flow and thickness of the particle surface. (Calero *et al.* 2009; Chen *et al.* 2012). The highest values of Thomas rate constant (K_{th}) at the lowest chromium ions concentration means the column adsorption system of the materials was kinetically favourable at lower levels of contamination (Suksabye *et al.* 2008). In the present study, the maximum solid phase concentration (q_0) decreased with the increase in the bed height because of the controlled rate step was shifted from external to internal mass transfer limitations and the model was competent to predict it. Thomas

Table 3 | Parameters predicted by Bohart-Adams and Thomas models at different bed heights, at neutral pH of chromium solution, a constant initial concentration and flow rate

C_0 (Initial concentration mg/L)	Bed height (cm), Z	Qv (Flow rate mL/min)	$K_{AB} \times 10^{-4}$ (L/mg min)	N_0 (mg/L)	R^2	Adj. R^2	RMSE
Bohart-Adams model							
10	5	0.5	26.14	123.49	0.946	0.932	0.231
10	10	0.5	30.20	121.88	0.915	0.902	0.121
10	15	0.5	33.77	114.36	0.961	0.953	0.223
C_0 (Initial concentration mg/L)	Bed height (cm), Z	Qv (Flow rate mL/min)	$K_{TH} \times 10^{-4}$ (L/min mg)	q_0 (mg/g)	R^2	Adj. R^2	RMSE
Thomas model							
10	5	0.5	24.1	466.2	0.971	0.966	0.359
10	10	0.5	25.8	347.6	0.988	0.986	0.222
10	15	0.5	29.7	272.3	0.997	0.992	0.213

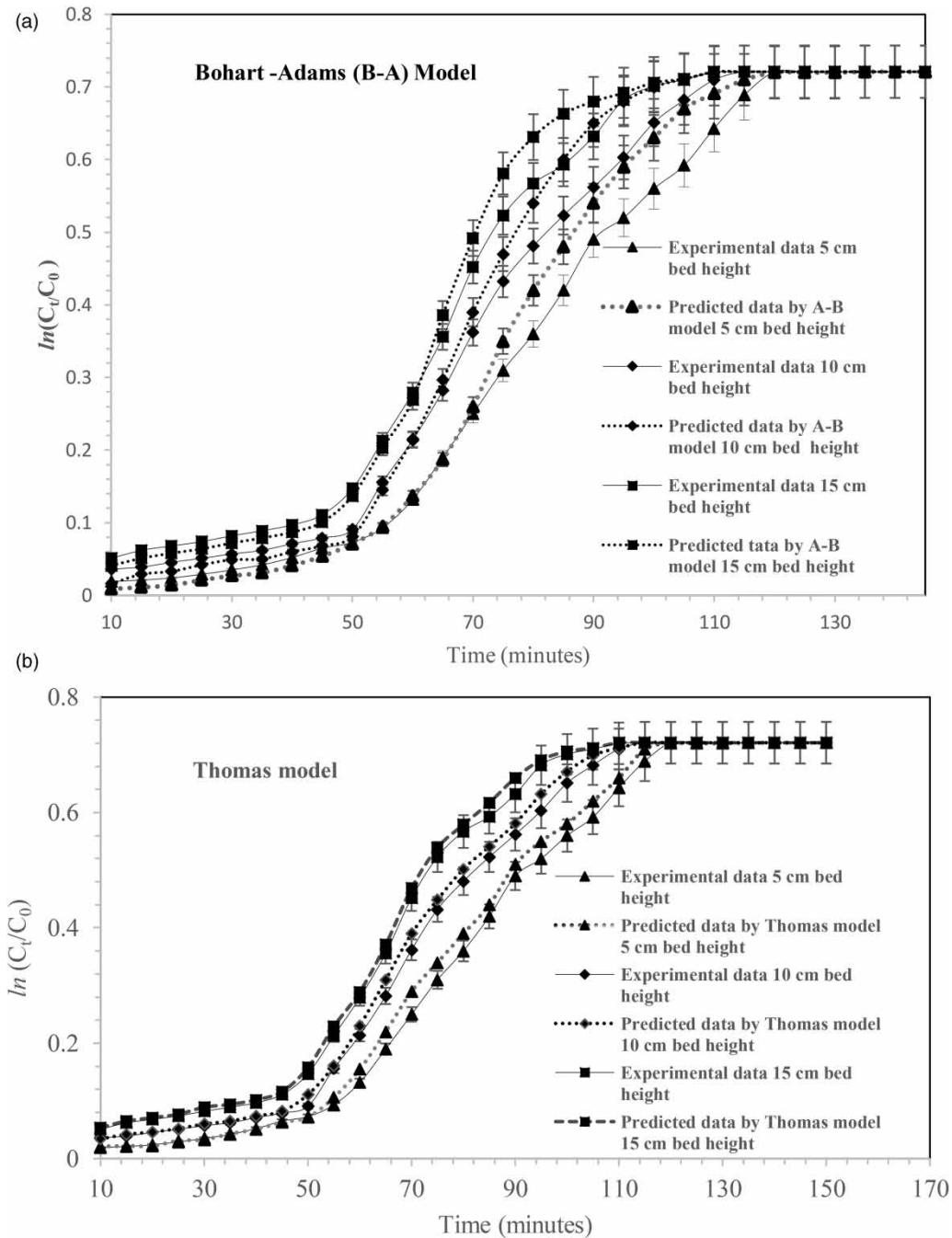


Figure 5 | Effect of bed height on Cr(VI) removal predicted by (a) Bohart-Adams model and (b) Thomas model.

model assumed Langmuir adsorption and second order reversible reaction kinetics was appropriate for adsorption processes (Yan *et al.* 2017).

CONCLUSION

The study concludes that the removal of hexavalent chromium in a fixed-bed column using activated charcoal derived from *S. trifoliolate* L fruit biomass is an effective and feasible method. Behaviour of breakthrough curve and the chromium adsorption capacity was found to be 1.719 mg/g which was strongly influenced by the bed height. Adsorption capacity was high at flow rate 0.5 mL/min, bed depth 15 cm, influent concentration 10 mg/L and pH 7. The prediction of breakthrough curve was

obtained by using Bohart-Adams and Thomas model. However, the entire breakthrough curve was best predicted by Thomas model. The length of the bed height strongly influenced the column breakthrough time and the adsorbent bed performance. The longer bed delayed the exhaustion time of the adsorbent, which indicated that the bed was capable to operate for a longer period without changing the adsorbent, while for the shorter bed, the exhaustion reached faster; therefore, the performance dropped. The breakthrough time also improved with increase in bed height.

ACKNOWLEDGEMENTS

The authors are thankful to Head of Department Environmental Science, Fakir Mohan University Balasore, Odisha, for necessary facilities and help in carry out the research work.

DATA AVAILABILITY STATEMENT

All relevant data are included in the paper or its Supplementary Information.

REFERENCES

- Baral, S. S., Das, S. N., Chaudhury, G. R., Swamy, Y. V. & Rath, P. 2008 Adsorption of Cr (VI) using thermally activated weed *Salvinia cucullata*. *Chem. Eng. J.* **139**, 245–255.
- Calero, M., Hernáinz, F., Blázquez, G., Tenorio, G. & Martín-Lara, M. A. 2009 Study of Cr(III) biosorption in a fixed-bed column. *J. Hazard. Mater.* **171**, 886–893.
- Chen, S., Yue, Q., Gao, B., Li, Q., Xu, X. & Fu, K. 2012 Adsorption of hexavalent chromium from aqueous solution by modified corn stalk: a fixed-bed column study. *Bioresour. Technol.* **113**, 114–120.
- Debnath, S., Biswas, K. & Ghosh, U. C. 2010 Removal of Ni(II) and Cr(VI) with Titanium(IV) oxide nanoparticle, agglomerates in fixed-bed columns. *Ind. Eng. Chem. Res.* **49**, 2031–2039.
- Dong, X., Ma, L. Q. & Li, Y. 2011 Characteristics and mechanisms of hexavalent chromium removal by biochar from sugar beet tailing. *J. Hazard. Mater.* **190** (1–3), 909–915.
- EPA 1990 *Environmental Protection Agency, Environmental Pollution Control Alternatives*. EPA/625/5-90/025, EPA/625/4-89/023, Cincinnati, OH, USA.
- Escudero, C., Fiol, N., Villaescusa, I. & Bollinger, J. C. 2017 Effect of chromium speciation on its sorption mechanism onto grape stalks entrapped into alginate beads. *Arabian J. Chem.* **10**, 1293–1302.
- Giri, A. K., Patel, R. & Mandal, S. 2012 Removal of Cr(VI) from aqueous solution by *Eichhornia crassipes* root biomass derived activated carbon. *Chem. Eng. J.* **185**, 71–81.
- Gorzin, F., Bahri, M. M. & Abadi, R. 2018 Adsorption of Cr(VI) from aqueous solution by adsorbent prepared from paper mill sludge: kinetics and thermodynamics studies. *Adsorpt. Sci. Technol.* **36** (1–2), 149–169.
- Greenberg, A. E., Trussell, R. R. & Clesceri, L. S. 2005 *Standard Methods for the Examination of Water and Wastewater*, 16th edn. APHA, AWWA, WPCF, Washington, DC, USA.
- Gupta, S. & Babu, B. V. 2009 Removal of toxic metal Cr(VI) from aqueous solutions using sawdust as adsorbent: equilibrium, kinetics and regeneration studies. *Chem. Eng. J.* **150** (2–3), 352–365.
- Kotas, J. & Stasicka, Z. 2000 Chromium occurrence in the environment and methods of its speciation. *Environ. Pollut.* **107**, 263–283.
- Nguyen, T. A. H., Ngo, H. H., Guo, W. S., Zhang, J., Liang, S., Yue, Q. Y., Li, Q. & Nguyen, T. V. 2013 Applicability of agricultural waste and by-products for adsorptive removal of heavy metals from wastewater. *Bioresour. Technol.* **148**, 574–585.
- Norouzi, S., Heidari, M., Alipour, V., Rahmanian, O., Fazizadeh, M., Mohammadi-Moghadam, F., Nourmoradi, H., Goudarzi, B. & Dindarloo, K. 2018 Preparation, characterization and Cr(VI) adsorption evaluation of NaOH-activated carbon produced from Date Press Cake; an agro-industrial waste. *Bioresour. Technol.* **258**, 48–56.
- Ortiz, I., Roman, M. F. S., Corvalan, S. M. & Eliceche, A. M. 2003 Modeling and optimization of an emulsion per traction process for removal and concentration of Cr (VI). *Ind. Eng. Chem. Res.* **42**, 5891–5899.
- Owalude, S. O. & Tella, A. C. 2016 Removal of hexavalent chromium from aqueous solutions by adsorption on modified groundnut hull. *Beni-suef Univ. J. Basic Appl. Sci.* **5** (4), 377–388.
- Saravanan, A., Senthil, K. P. & Yashwanthraj, M. 2017 Sequestration of toxic Cr(VI) ions from industrial wastewater using waste biomass: a review. *Desalin. Water Treat.* **68**, 245–266.
- Sawalha, M. F., Peralta-Videa, J. R., Saupé, G. B., Dokken, K. M. & Gardea-Torresdey, J. L. 2007 Using FTIR to corroborate the identity of functional groups involved in the binding of Cd and Cr to saltbush (*Atriplex canescens*) biomass. *Chemosphere* **66** (8), 1424–1430.
- Sharaf EI-Deen, S. E. A. & Sharaf EI-Dean, G. E. 2015 Adsorption of Cr(VI) from aqueous solution by activated carbon prepared from agricultural solid waste. *Sep. Sci. Technol.* **50** (10), 1469–1479.
- Singha, B. & Das, S. K. 2011 Biosorption of Cr(VI) ions from aqueous solutions: kinetics, equilibrium, thermodynamics and desorption studies. *Colloids Surf. B* **84**, 221–232.

- Suksabye, P., Thiravetyan, P. & Nakbanpote, W. 2008 Column study of chromium (VI) adsorption from electroplating industry by coconut coir pith. *J. Hazard. Mater.* **160**, 56–62.
- Tu, B., Wen, R., Wang, K., Cheng, Y., Cao, Y. D. W., Zhang, K. & Tao, H. 2020 Efficient removal of aqueous hexavalent chromium by activated carbon derived from Bermuda grass. *J. Colloid Interface Sci.* **560**, 649–658.
- Yan, Y., An, Q., Xiao, Z., Zheng, W. & Zhai, S. 2017 Flexible core shell/bead like alginate@PEI with exceptional adsorption capacity, recycling performance toward batch and column sorption of Cr(VI). *Chem. Eng. J.* **313**, 475–486.
- Yang, J., Yu, M. & Chen, W. 2015 Adsorption of hexavalent chromium from aqueous solution by activated carbon prepared from longan seed: kinetics, equilibrium and thermodynamics. *J. Ind. Eng. Chem.* **21** (25), 414–422.

First received 18 January 2021; accepted in revised form 21 May 2021. Available online 8 June 2021